

Statistical time series methods for damage diagnosis in a scale aircraft skeleton structure: loosened bolts damage scenarios

Fotis P Kopsaftopoulos and Spilios D Fassois¹

Stochastic Mechanical Systems & Automation (SMSA) Laboratory
Department of Mechanical & Aeronautical Engineering
University of Patras, GR 265 00 Patras, Greece
URL: <http://www.smsa.upatras.gr>

E-mail: fkopsaf@mech.upatras.gr, fassois@mech.upatras.gr

Abstract. A comparative assessment of several vibration based statistical time series methods for Structural Health Monitoring (SHM) is presented via their application to a scale aircraft skeleton laboratory structure. A brief overview of the methods, which are either scalar or vector type, non-parametric or parametric, and pertain to either the response-only or excitation-response cases, is provided. Damage diagnosis, including both the detection and identification subproblems, is tackled via scalar or vector vibration signals. The methods' effectiveness is assessed via repeated experiments under various damage scenarios, with each scenario corresponding to the loosening of one or more selected bolts. The results of the study confirm the "global" damage detection capability and effectiveness of statistical time series methods for SHM.

1. Introduction

Statistical time series methods for damage detection and identification (localization), collectively referred to as damage diagnosis, utilize random excitation and/or vibration response signals, along with statistical model building and decision making tools, for inferring the health state of a structure (Structural Health Monitoring – SHM). They offer a number of advantages, including no requirement for physics based or finite element models, no requirement for complete modal models, effective treatment of uncertainties, and statistical decision making with specified performance characteristics [1,2]. These methods form an important and useful category within the broader family of vibration based methods for SHM [3,4].

Statistical time series methods for SHM are based on *scalar* or *vector* stochastic vibration signals, identification of suitable (parametric or non-parametric) time series models describing the dynamics in each structural state, and extraction of a statistical characteristic quantity Q characterizing the structural state in each case (baseline phase). Damage diagnosis is then accomplished via statistical decision making consisting of comparing, in a statistical sense, the current characteristic quantity Q_u with that of each potential state as determined in the baseline

¹Corresponding author. Tel/Fax: (+30) 2610 969 495 (direct); 969 492 (central)

phase (inspection phase). For an overview of the basic principles and the main statistical time series methods for SHM the interested reader is referred to [1,2]. An experimental assessment of several methods is provided in [5]. Non-parametric methods are those based on non-parametric time series representations, such as the spectral density function [1,2], and have received limited attention in the literature [5–7]. Parametric time series methods are those based on parametric time series representations, such as the AutoRegressive Moving Average (ARMA) models [1,2]. This latter category has attracted increased attention recently [5, 8–11], with approaches for accounting for varying environmental conditions being also considered [10,11].

The *goal* of the present study is the comparative assessment of several *scalar* (univariate) and *vector* (multivariate) statistical time series methods for SHM, both of the non-parametric and parametric types, via their application to an aircraft scale skeleton laboratory structure. A related assessment of many methods may be found in a recent work by the authors [12]. The present study is an extension that also presents results with an additional, statistically optimal, method based on the Sequential Probability Ratio Test (SPRT) [13,14]. In this work four scalar methods, namely a Power Spectral Density (PSD), a Frequency Response Function (FRF), a model residual variance, and a Sequential Probability Ratio Test (SPRT) based method are employed, along with two vector methods, namely a model parameter based and a likelihood function based method. A large number of experiments are run and a number of damage scenarios are considered, with each one corresponding to the loosening of one or more bolts at various positions on the structure.

The main issues the study addresses include: (i) comparison of the performance of *scalar* and *vector* statistical time series methods with regard to effective damage diagnosis – false alarms, missed damage, and damage misclassification rates are investigated using many experiments; (ii) assessment of the methods in terms of their *detection* and *identification* (localization) capabilities under various scenarios with respect to *single* or *multiple* vibration signal measurements and the use of “local” or “remote” (in relation to the damage position) sensors.

2. The structure and the experimental set-up

2.1. The structure

The scale aircraft skeleton laboratory structure was designed by ONERA in conjunction with the GARTEUR SM-AG19 Group and manufactured at the University of Patras (figure 1). It represents a typical, basic, aircraft skeleton design and consists of six solid beams with rectangular cross sections representing the fuselage ($1500 \times 150 \times 50$ mm), the wing ($2000 \times 100 \times 10$ mm), the horizontal ($300 \times 100 \times 10$ mm) and vertical stabilizers ($400 \times 100 \times 10$ mm), and the right and left wing-tips ($400 \times 100 \times 10$ mm). All parts are constructed from standard aluminum and are jointed together via steel plates and bolts. The total mass of the structure is 50 kg.

2.2. The damage types and the experiments

Damage detection and identification are based on vibration testing of the structure, which is suspended through a set of bungee cords and hooks from a long rigid beam sustained by two heavy-type stands (figure 1). The suspension is designed in a way as to exhibit a pendulum rigid body mode below the frequency range of interest, as the boundary conditions are free-free.

The excitation is broadband random stationary Gaussian applied vertically at the right wing-tip (Point X, figure 1) through an electromechanical shaker (MB Dynamics Modal 50A, max load 225 N). The actual force exerted on the structure is measured via an impedance head (PCB M288D01), while the resulting vertical acceleration responses at Points Y1–Y4 (figure 1) are measured via lightweight accelerometers (PCB 352A10). The force and acceleration signals are driven through a conditioning charge amplifier (PCB 481A02) into the data acquisition system based on SigLab 20–42 measurement modules. The damage scenarios used in the study

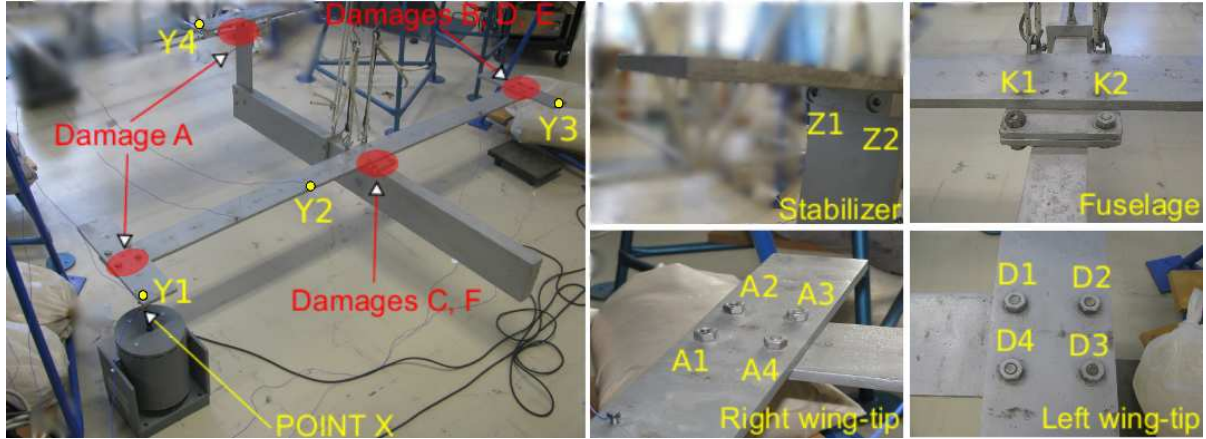


Figure 1. The aircraft scale skeleton structure and the experimental set-up: The force excitation (Point X), the vibration measurement locations (Points Y1–Y4), and the bolts connecting the various elements of the structure.

correspond to the *complete loosening* of one or more bolts at different joints of the structure (figure 1). Six distinct types (designated as A, B, . . . , F) are considered and are summarized in table 1.

The assessment of the methods with respect to the damage detection and identification subproblems is based on 60 inspection experiments for the healthy state and 40 experiments for each considered damage state (damage types A, B, . . . , F – see table 1). In each experiment *four* vibration measurement locations (figure 1, Points Y1–Y4) are used in order to allow diagnosis with one or more vibration response signals. For damage detection a single healthy data set is used for establishing the baseline (reference) model. Similarly, for damage identification a single data set for each damage scenario (damage types A, B, . . . , F) is used for establishing the corresponding baseline (reference) model.

2.3. Identified structural dynamics for the healthy structure

Non-parametric identification is based on $N = 46\,080$ (≈ 90 s) sample-long excitation–response signals obtained from the *four* vibration measurement locations on the structure (figure 1). An $L = 2048$ sample-long Hamming data window with zero overlap is used (number of segments

Table 1. The damage scenarios (types) and experimental details

Structural state	Description	No of inspection experiments
Healthy	—	60
Damage A	loosening of bolts A1, A4, Z1, Z2	40
Damage B	loosening of bolts D1, D2, D3	40
Damage C	loosening of bolts K1	40
Damage D	loosening of bolts D2, D3	40
Damage E	loosening of bolts D3	40
Damage F	loosening of bolts K1, K2	40

Sampling frequency: $f_s = 512$ Hz, Signal bandwidth: $[4 - 200]$ Hz
Non-parametric methods: $N = 46\,080$ samples (90 s); Parametric methods: $N = 15\,000$ samples (29 s)

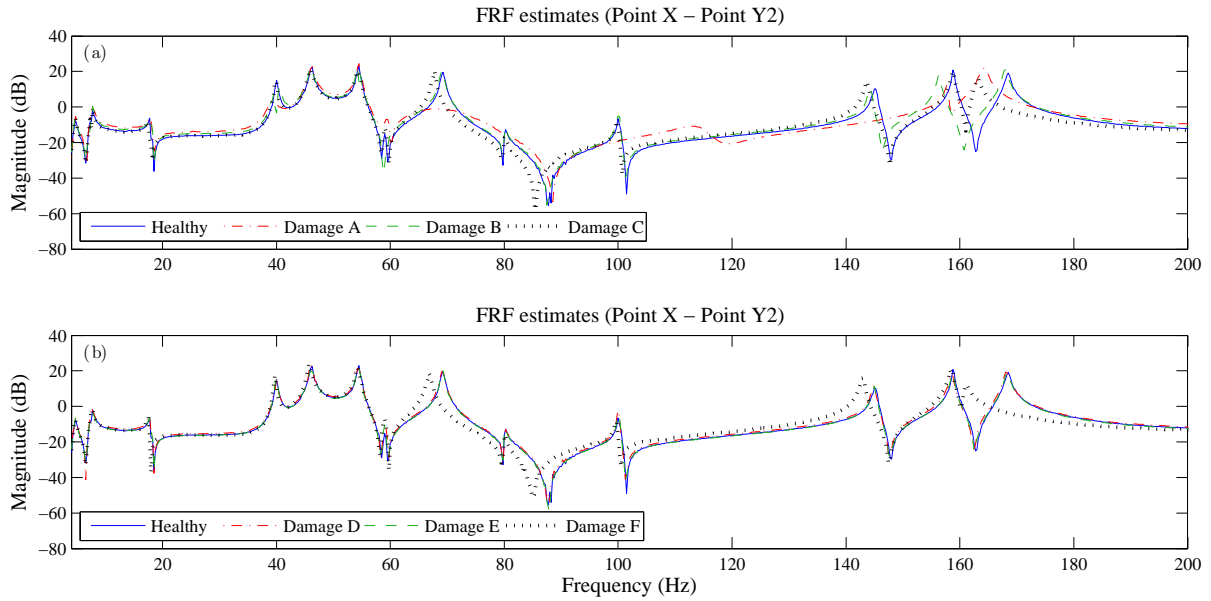


Figure 2. Non-parametric Welch-based estimates of the frequency response function (FRF) magnitude for the healthy and damage structural states (single experiment per case; Point X – Point Y2 transfer function).

$K = 22$) for Welch-based PSD (MATLAB function *pwelch.m*) and FRF (MATLAB function *tfestimate.m*) estimation (table 2). The obtained FRF estimates, corresponding to the healthy and damage states of the structure, for the Point X – Point Y2 transfer function are depicted in figure 2. Observe that discrepancies among the various cases are observed for some damage cases, but seem to be rather small for certain of them.

Parametric identification of the structural dynamics is based on $N = 15\,000$ (≈ 29 s) sample-long excitation and response signals which are used for estimating Vector AutoRegressive with eXogenous excitation (VARX(n_a, n_b)) models (MATLAB function *arx.m*). Model parameter estimation is achieved by minimizing a quadratic Prediction Error (PE) criterion leading to a Least Squares (LS) type estimator [15], [16, p. 206]. Model order selection is based on a combination of tools, including the Bayesian Information Criterion (BIC) [15], [16, pp. 505–507] and “stabilization diagrams” (which depict the estimated modal parameters, usually frequencies, as a function of increasing model order [15]). In this case, BIC minimization is achieved for orders $n_a = n_b = 80$, thus a 4-variate VARX(80,80) model is presently selected as adequate (Samples Per Parameter (SPP) ratio 37.4).

Table 2. Non-parametric estimation details

Data length	$N = 46\,080$ samples (≈ 90 s)
Method	Welch
Segment length	$L = 2\,048$ samples
No of non-overlapping segments	$K = 22$
Window type	Hamming
Frequency resolution	$\Delta f = 0.25$ Hz

3. Statistical time series methods for SHM

Statistical time series methods for SHM employ *scalar* (univariate) or *vector* (multivariate) random excitation and/or response signals. Despite their phenomenal resemblance to their univariate counterparts, multivariate models have a much richer structure while the corresponding methods require multivariate statistical decision making procedures [2], [17, Chapters 3, 4].

3.1. Scalar methods

Two non-parametric, namely a Power Spectral Density (PSD) and a Frequency Response Function (FRF) based method, and two parametric, namely a residual variance, and a Sequential Probability Ratio Test (SPRT) based method, scalar methods are briefly reviewed. Their main characteristics are summarized in table 3.

3.1.1. Power Spectral Density (PSD) based method. Damage detection and identification is in this case tackled via changes in the PSD of the measured vibration response signals (non-parametric method). The excitation is assumed unavailable (response-only case). The method's characteristic quantity is the PSD function $Q = S(\omega)$ (ω designating frequency – table 3). Damage detection is based on confirmation of statistically significant deviations from the nominal healthy case at some frequency [1,2]. Damage identification may be achieved by performing hypothesis tests comparing the current PSD to those corresponding to different damage types and obtained in the baseline phase.

3.1.2. Frequency Response Function (FRF) based method. This is similar to the PSD method, except that it requires the availability of both the excitation and response signals (excitation-response case) and uses the FRF magnitude as its characteristic quantity (non-parametric method), thus $Q = |H(j\omega)|$ (table 3). The main idea is the comparison of the FRF magnitude of the current structural state to that of the healthy structure. Damage detection is based on confirmation of statistically significant deviations from the nominal healthy case at some frequency [1,2]. Damage identification may be achieved similarly to the previous case.

3.1.3. Residual variance based method. In this method the characteristic quantity is the residual variance (table 3). The main idea is based on the fact that the model (parametric method) matching the current state of the structure should generate a residual sequence characterized by minimal variance [1,2]. Thus damage detection may be achieved by examining whether or not the residual variance is minimal [1,2]. The method uses classical tests on the residuals and offers simplicity and no need for model estimation in the inspection phase.

3.1.4. Sequential Probability Ratio Test (SPRT) based method. This method employs the Sequential Probability Ratio Test (SPRT) [13] [14, Chapter 3] in order to detect a change in the standard deviation σ of the model (parametric method) residual sequence ($e[t] \sim \mathcal{N}(0, \sigma^2)$, $t = 1, \dots, N$). An SPRT of strength (α, β) , with α, β the type I (false alarm) and II (missed damage) error probabilities, respectively, is used for the following hypothesis testing problem:

$$\begin{aligned} H_o & : \sigma_{ou} \leq \sigma_o && \text{(null hypothesis – healthy structure)} \\ H_1 & : \sigma_{ou} \geq \sigma_1 && \text{(alternative hypothesis – damaged structure)} \end{aligned} \quad (1)$$

with σ_o, σ_1 designating user defined values. The basis of the SPRT is the logarithm of the likelihood ratio function based on n samples:

$$\mathcal{L}(n) = \log \frac{f(e[1], \dots, e[n]|H_1)}{f(e[1], \dots, e[n]|H_o)} = \sum_{t=1}^n \log \frac{f(e[t]|H_1)}{f(e[t]|H_o)} = n \cdot \log \frac{\sigma_o}{\sigma_1} + \frac{\sigma_1^2 - \sigma_o^2}{2\sigma_o^2\sigma_1^2} \cdot \sum_{t=1}^n e^2[t] \quad (2)$$

Table 3. Characteristics of the employed statistical time series methods for SHM

Method	Principle	Test Statistic	Type
PSD based	$S_u(\omega) \stackrel{?}{=} S_o(\omega)$	$F = \widehat{S}_o(\omega)/\widehat{S}_u(\omega) \sim F(2K, 2K)$	scalar
FRF based	$\delta H(j\omega) = H_o(j\omega) - H_u(j\omega) \stackrel{?}{=} 0$	$Z = \delta \widehat{H}(j\omega) /\sqrt{2\widehat{\sigma}_H^2(\omega)} \sim N(0, 1)$	scalar
Residual variance	$\sigma_{ou}^2 \stackrel{?}{\leq} \sigma_{oo}^2$	$F = \widehat{\sigma}_{ou}^2/\widehat{\sigma}_{oo}^2 \sim F(N, N - d)$	scalar
SPRT based	$\sigma_{ou} \stackrel{?}{\leq} \sigma_o$ or $\sigma_{ou} \stackrel{?}{\geq} \sigma_1$	$\mathcal{L}(n) = n \cdot \log \frac{\sigma_o}{\sigma_1} + \frac{\sigma_1^2 - \sigma_o^2}{2\sigma_o^2\sigma_1^2} \cdot \sum_{t=1}^n e^2[t]$	scalar
Model parameter	$\delta\boldsymbol{\theta} = \boldsymbol{\theta}_o - \boldsymbol{\theta}_u \stackrel{?}{=} \mathbf{0}$	$\chi_\theta^2 = \delta\widehat{\boldsymbol{\theta}}^T (2\widehat{\mathbf{P}}_\theta)^{-1} \delta\widehat{\boldsymbol{\theta}} \sim \chi^2(d)$	vector
Residual likelihood	$\boldsymbol{\theta}_o \stackrel{?}{=} \boldsymbol{\theta}_u$	$\sum_{t=1}^N (\mathbf{e}_u^T[t, \boldsymbol{\theta}_o] \cdot \boldsymbol{\Sigma}_o \cdot \mathbf{e}_u[t, \boldsymbol{\theta}_o]) \leq l$	vector

$S(\omega)$: Power Spectral Density (PSD) function; $|H(j\omega)|$: Frequency Response Function (FRF) magnitude
 $\sigma_H^2(\omega) = \text{var} [|\widehat{H}_o(j\omega)|]$; $\boldsymbol{\theta}$: model parameter vector; d : parameter vector dimensionality; \mathbf{P}_θ : covariance of $\boldsymbol{\theta}_o$
 σ_{oo}^2 : variance of residual signal obtained by driving the healthy structure signals through the healthy model
 σ_{ou}^2 : variance of residual signal obtained by driving the current structure signals through the healthy model
 σ_o, σ_1 : user defined values for the residual standard deviation under healthy and damage states, respectively
 \mathbf{e} : k -variate residual sequence; $\boldsymbol{\Sigma}$: residual covariance matrix; l : user defined threshold
The subscripts “o” and “u” designate the healthy and current (unknown) structural states, respectively.

with $\mathcal{L}(n)$ designating the decision parameter of the method and $f(e[t]|H_i)$ the probability density function (normal distribution) of the residual sequence under H_i ($i = 0, 1$).

The following test is then constructed at the (α, β) risk levels:

$$\begin{aligned}
 \mathcal{L}(n) \leq B &\implies H_o \text{ is accepted} && \text{(healthy structure)} \\
 \mathcal{L}(n) \geq A &\implies H_1 \text{ is accepted} && \text{(damaged structure)} \\
 B < \mathcal{L}(n) < A &\implies \text{no decision is made} && \text{(continue the test)}
 \end{aligned} \tag{3}$$

with $B = \beta/(1 - \alpha)$ and $A = (1 - \beta)/\alpha$. Following a decision, $\mathcal{L}(n)$ is reset to zero.

Damage identification may be achieved by performing SPRTs similar to the above separately for damages of each potential type.

3.2. Vector methods

Two *vector* (multivariate) parametric time series methods for SHM, namely a model parameter based method and a residual likelihood function based method, are briefly reviewed. The main characteristics of the methods are also summarized in table 3.

3.2.1. A model parameter based method. This method bases damage detection and identification on a characteristic quantity Q which is a function of the parameter vector $\boldsymbol{\theta}$ of a parametric time series model (parametric method – see table 3) [1, 2]. The model has to be re-estimated in the inspection phase based on signals from the current (unknown) state of the structure. Damage detection is based on testing for statistically significant changes in the parameter vector $\boldsymbol{\theta}$ between the nominal and current structures through a hypothesis testing problem. Damage identification may be based on multiple hypothesis testing comparing the current parameter vector to those corresponding to different damage types.

3.2.2. Residual likelihood function based method. Damage detection is based on the likelihood function evaluated for the current signal(s) under each one of the considered structural states [1, 2]. The hypothesis corresponding to the largest likelihood is selected as that representing the current structural state (table 3).

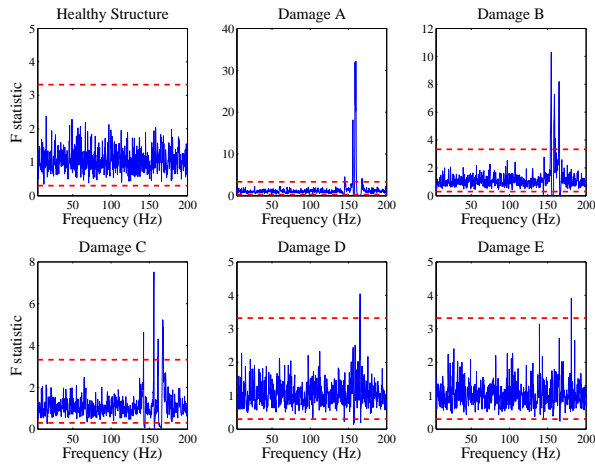


Figure 3. PSD based method: Indicative damage detection results (sensor Y1) at the $\alpha = 10^{-4}$ risk level. The actual structural state is shown above each plot.

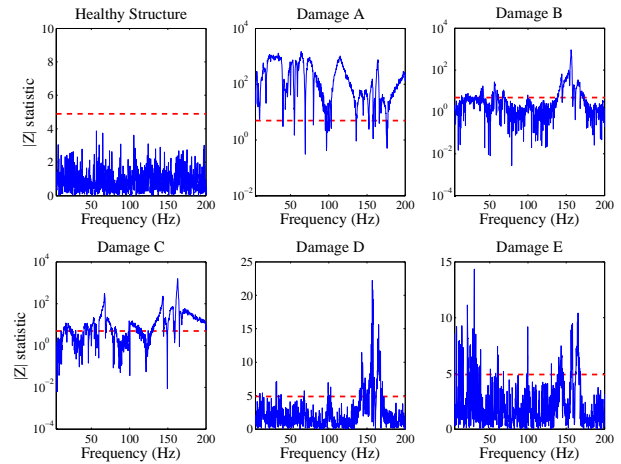


Figure 4. FRF based method: Indicative damage detection results (sensor Y4) at the $\alpha = 10^{-6}$ risk level. The actual structural state is shown above each plot.

4. Experimental damage detection and identification results

4.1. Scalar methods

4.1.1. Power Spectral Density (PSD) based method. Typical damage detection results, obtained from response (sensor) Y1 are presented in figure 3. Evidently, correct detection at the $\alpha = 10^{-4}$ risk level is obtained in each case, as the test statistic is shown not to exceed the critical points (dashed horizontal lines) in the healthy case, while it exceeds them in each damage case. Observe that damage types A, B and C (see figure 1 and table 1) appear easier to detect, while damage types D and E harder. Summary damage detection and identification results for all four vibration measurement locations are presented in table 4. The PSD based method achieves accurate damage detection as no false alarms are exhibited, while the number of missed damage cases is zero for all damage scenarios. The method is also capable of identifying the actual damage type; zero damage misclassification errors are reported for damage types A, C, D and F, several are reported for damage type B, and a few for damage type E. The misclassification problem is more intense for damage type B when the Y3 and Y4 vibration measurement locations (sensors) are used.

4.1.2. Frequency Response Function (FRF) based method. Figure 4 presents typical damage detection results with the FRF based method and response (sensor) Y4. Correct detection at the $\alpha = 10^{-6}$ risk level is achieved in each case, as the test statistic is shown not to exceed the critical point (dashed horizontal line) in the healthy case, while it exceeds it in all damage cases. Again, damage types A, B and C appear easier to detect (note the logarithmic scale at the vertical axis in figure 4), while damage types D and E appear harder. The summarized damage detection and identification results for all vibration measurement locations are presented in table 4. The method achieves effective damage detection, as no false alarms or missed damages are reported, but has problems with damage identification as several misclassification errors are reported for damage types B, C, and D.

4.1.3. Residual variance based method. The residual variance based method is based on the identified 4-variate VARX(80,80) models obtained in the baseline phase, as well as on the current (unknown) data records. Damage detection and identification is achieved via statistical comparison of the two residual variances (each one of the scalar responses is considered

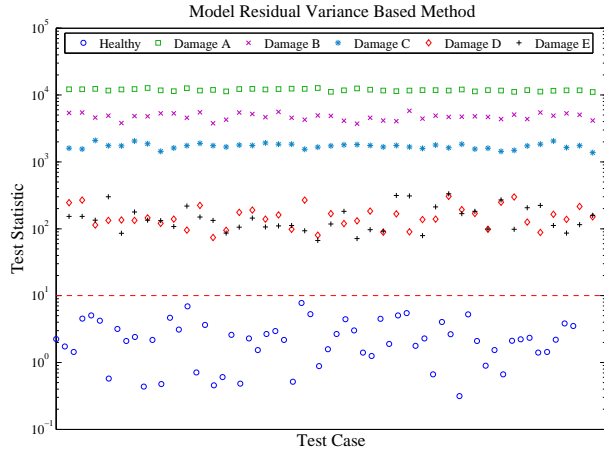


Figure 5. Residual variance based method: Damage detection results (sensor Y2) – each mark represents an experiment (60 healthy experiments; 200 damage experiments). A damage is detected if the test statistic exceeds the critical point.

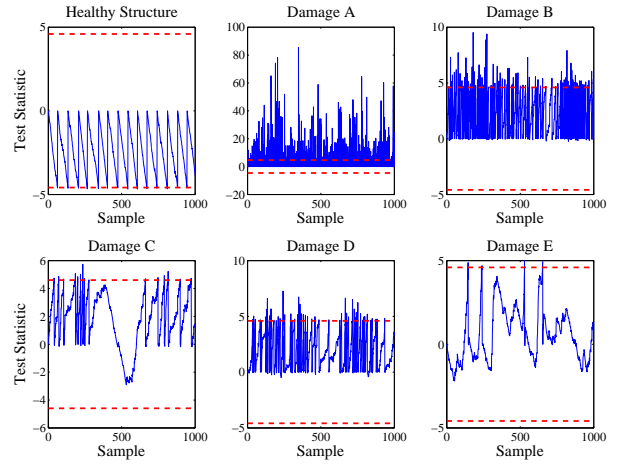


Figure 6. SPRT based method: Indicative damage detection results (sensor Y1) at the $\alpha = \beta = 0.01$ risk levels ($\sigma_1/\sigma_o = 1.1$). The actual structural state is shown above each plot.

separately). Typical damage detection results are shown in figure 5. Correct detection is obtained in each considered case, as the test statistic is shown not to exceed the critical point in the healthy case, while it exceeds it in all of the damage cases. Summary damage detection and identification results for the considered vibration measurement locations are presented in table 4. The method achieves effective damage detection and identification as no false alarms, missed damages, or damage misclassification errors cases are observed.

4.1.4. Sequential Probability Ratio Test (SPRT) based method. The SPRT based method employs the identified 4-variate VARX(80,80) models obtained in the baseline phase, as well as the current (unknown) data records. Damage detection and identification is achieved via statistical comparison of the two residual standard deviations using the SPRT (each one of the scalar responses is considered separately). The nominal residual standard deviation σ_o is selected as the mean standard deviation of the residuals obtained from the 60 healthy data sets driven through the baseline healthy VARX(80,80) model. The residual standard deviation ratio σ_1/σ_o is chosen equal to 1.1 (see equations 1 and 2).

Typical damage detection results at the $\alpha = \beta = 0.01$ risk levels obtained via the SPRT based method for vibration response (sensor) Y1 are shown in figure 6. A damage is detected when the test statistic exceeds the upper critical point (dashed horizontal lines), while the structure is determined to be in its healthy state when the test statistic lies below the lower critical point. After a decision is made, the test statistic is reset to zero and the test continues, thus during testing multiple decisions are made. Evidently, correct detection (figure 6) is obtained in each considered case, as the test statistic is shown to lie below the lower critical point in the healthy case, while it exceeds the upper critical point in the damage test cases. Observe that damage types A and B (table 1) appear easier to detect, while damage types C and E appear harder. Summary results for all vibration measurement locations are presented in table 4. The method exhibits excellent performance in damage detection and identification as no false alarms, missed damages, or damage misclassification errors are observed.

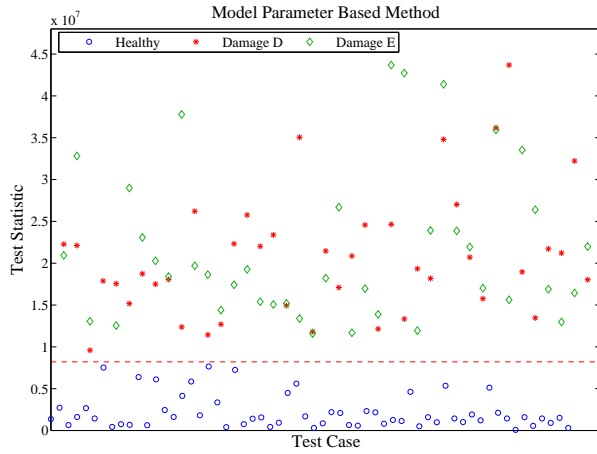


Figure 7. Model parameter based method: Damage detection results for three structural states. Each mark represents an experiment (60 healthy experiments; 80 damage experiments). A damage is detected if the test statistic exceeds the critical point.

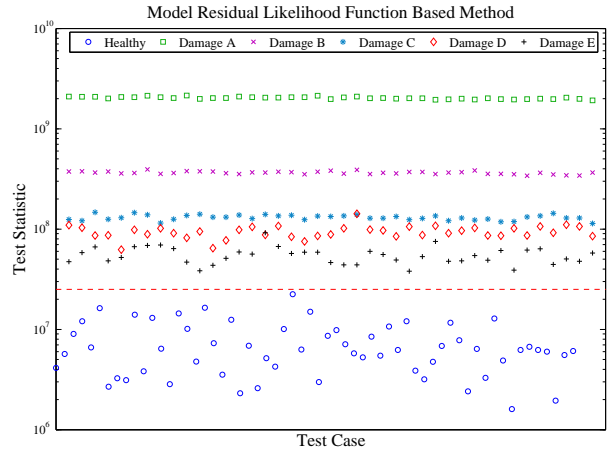


Figure 8. Residual likelihood function based method: Damage detection results. Each mark represents an experiment (60 healthy experiments; 200 damage experiments). A damage is detected if the test statistic exceeds the critical point.

4.2. Vector methods

4.2.1. Model parameter based method. This method also employs the identified in the baseline phase 4-variate VARX(80,80) models, as well as an identified VARX(80,80) model for each current data record (all measured response signals are simultaneously employed). Figure 7 presents typical damage detection results. The healthy test statistics are shown in circles (60 experiments), while the “least severe” damage types D and E are presented with asterisks and diamonds, respectively (one for each one of the 40 experiments). Evidently, correct detection is obtained in each case, as the test statistic is shown not to exceed the critical point in the healthy cases, while it exceeds it in the damage cases. As table 5 indicates, the method achieves accurate damage detection and identification, as no false alarm, missed damage, or damage misclassification errors are reported.

4.2.2. Residual likelihood function based method. The residual likelihood function based method is based on the identified in the baseline phase 4-variate VARX(80,80) models. Figure 8 presents typical damage detection results. Correct detection is obtained in each case, as the test statistic is shown not to exceed the critical point in the healthy cases, while it exceeds it in all damage cases. The method achieves accurate damage detection and identification, as no false alarm, missed damage, or damage misclassification errors are reported (summary results in table 5).

5. Concluding remarks

Both scalar and vector statistical time series methods for SHM were shown to effectively tackle damage detection and identification, with the vector methods achieving excellent performance with zero false alarm, missed damage, and damage misclassification rates. Moreover, both types of methods have “global” damage detection capability, as they are able to detect “local” and “remote” damage with respect to the sensor location being used, while they are also able to correctly identify the actual damage type. A notable exception has been the FRF based method which exhibited an increased number of damage misclassification errors for three damage types. Vector parametric time series methods are more elaborate and require higher user expertise, yet

Table 4. Scalar methods: damage detection and identification summary results

Method	Damage Detection						
	False alarms	Missed damage					
		damage A	damage B	damage C	damage D	damage E	damage F
PSD based	0/0/0/0	0/0/0/0	0/0/0/0	0/0/0/0	0/0/0/0	0/0/0/0	0/0/0/0
FRF based	1/0/0/ 35	0/0/0/0	0/0/0/0	0/0/0/0	0/0/1/0	0/1/0/0	0/0/0/0
Res. variance [†]	0/0/0/0	0/0/0/0	0/0/0/0	0/0/0/0	0/0/0/0	0/0/0/0	0/0/0/0
SPRT based	0/0/0/0	0/0/0/0	0/0/0/0	0/0/0/0	0/0/0/0	0/0/0/0	0/0/0/0

False alarms for response points Y1/Y2/Y3/Y4 out of 60 test cases per point.

Missed damages for response points Y1/Y2/Y3/Y4 out of 40 test cases per point; [†]adjusted α .

Method	Damage Identification					
	Damage misclassification					
	damage A	damage B	damage C	damage D	damage E	damage F
PSD based	0/0/0/0	0/0/21/21	0/0/0/0	0/0/0/0	0/0/1/2	0/0/0/0
FRF based	0/0/0/0	10/4/7/8	6/10/2/0	5/22/9/8	2/9/5/2	0/3/1/0
Res. variance [†]	0/0/0/0	0/0/0/0	0/0/0/0	0/0/0/0	0/0/0/0	0/0/0/0
SPRT based	0/0/0/0	0/0/0/0	0/0/0/0	0/0/0/0	0/0/0/0	0/0/0/0

Damage misclassification for response points Y1/Y2/Y3/Y4 out of 40 test cases per point; [†]adjusted α .

Table 5. Vector methods: damage detection and identification summary results

Method	Damage Detection							Damage Identification					
	False alarms	Missed damage						Damage misclassification					
		dam A	dam B	dam C	dam D	dam E	dam F	dam A	dam B	dam C	dam D	dam E	dam F
Mod. par. [†]	0	0	0	0	0	0	0	0	0	0	0	0	0
Res. lik. [†]	0	0	0	0	0	0	0	0	0	0	0	0	0

False alarms out of 60 test cases. **Missed damages** out of 40 test cases.

Damage misclassification out of 40 test cases; [†]adjusted α .

they seem to offer potentially enhanced performance.

References

- [1] Fassois S D and Sakellariou J S 2007 *Philos. T. Roy. Soc. A* **365** 411–448
- [2] Fassois S D and Sakellariou J S 2009 *Encyclopedia of Structural Health Monitoring* ed Boller C, Chang F K and Fujino Y (John Wiley & Sons Ltd.) pp 443–472
- [3] Sakellariou J S and Fassois S D 2008 *Mech. Syst. Signal Pr.* **22** 557–573
- [4] Kopsaftopoulos F P and Fassois S D 2007 *Key Eng. Mat.* **347** 127–132
- [5] Kopsaftopoulos F P and Fassois S D 2010 *Mech. Syst. Signal Pr.* **24** 1977–1997
- [6] Sakellariou J S, Petsounis K A and Fassois S D 2001 *Proc. of First Nat. Conf. on Recent Advances in Mechanical Engineering* (Patras, Greece)
- [7] Rizos D D, Fassois S D, Marioli-Riga Z P and Karanika A N 2008 *Mech. Syst. Signal Pr.* **22** 315–337
- [8] Sohn H and Farrar C R 2001 *Smart Mater. Struct.* **10** 446–451
- [9] Carden E P and Brownjohn J M 2008 *Mech. Syst. Signal Pr.* **22** 295–314
- [10] Hios J D and Fassois S D 2009 *Key Eng. Mat.* **413–414** 261–268
- [11] Lekkas A M, Hios J D and Fassois S D 2010 *Proc. of the 5th European Workshop on SHM* (Sorrento, Italy)
- [12] Kopsaftopoulos F P, Magripis S G, Amlianitis A D and Fassois S D 2010 *Proc. of the ASME 2010 10th Biennial Conf. on Engineering Systems Design and Analysis* (Istanbul, Turkey)
- [13] Wald A 2004 *Sequential Analysis* (New York: Dover Publications Inc.)
- [14] Ghosh B K and Sen P K (eds) 1991 *Handbook of Sequential Analysis* (New York: Marcel Dekker, Inc.)
- [15] Fassois S D 2001 *Encyclopedia of Vibration* ed Braun S, Ewins D and Rao S (Academic Press) pp 673–685
- [16] Ljung L 1999 *System Identification: Theory for the User* 2nd ed (Prentice-Hall)
- [17] Lütkepohl H 2005 *New Introduction to Multiple Time Series Analysis* (Springer-Verlag Berlin)